

Scalar-on-Image Regression via the Soft-Thresholded Gaussian Process

Jian Kang*, Brian J. Reich and Ana-Maria Staicu

Abstract

The focus of this work is on spatial variable selection for scalar-on-image regression. We propose a new class of Bayesian nonparametric models, soft-thresholded Gaussian processes and develop the efficient posterior computation algorithms. Theoretically, soft-thresholded Gaussian processes provide large prior support for the spatially varying coefficients that enjoy piecewise smoothness, sparsity and continuity, characterizing the important features of imaging data. Also, under some mild regularity conditions, the soft-thresholded Gaussian process leads to the posterior consistency for both parameter estimation and variable selection for scalar-on-image regression, even when the number of true predictors is larger than the sample size. The proposed method is illustrated via simulations, compared numerically with existing alternatives and applied to Electroencephalography (EEG) study of alcoholism.

Keywords: spatial variable selection, EEG, posterior consistency, Gaussian processes.

*Jian Kang is Assistant Professor in the Department of Biostatistics, University of Michigan, Ann Arbor, MI 48019. Email: jiankang@umich.edu. Brian J. Reich is Associated Professor Department of Statistics, North Carolina State University, Raleigh, NC 27695. Email: bjreich@ncsu.edu. Ana-Maria Staicu is Associated Professor Department of Statistics, North Carolina State University, Raleigh, NC 27695. Email: astaicu@ncsu.edu

1 Introduction

Scalar-on-image regression has attracted considerable attention recently in both frequentist and Bayesian literature. This problem is challenging for several reasons such as: 1) the predictor is very high dimensional (two dimensional or three dimensional image), often larger than the sample size, 2) the observed predictor may be contaminated with noise and the true predictor signal may exhibit complex correlation structure, and 3) most components of the predictor may have no effect on the response, and when they have an effect it may vary smoothly.

Regularized regression techniques are usually needed when the dimension of the predictor is much higher relative to the sample size; lasso (Tibshirani 1996) is a popular method for variable selection by employing a penalty based on the sum of the absolute values of the regression coefficients. However most approaches do not accommodate predictors with ordered components such as in the case of predictor images. One exception is the fused lasso, which generalizes the lasso by penalizing both the coefficients and their successive differences, thus ensuring both sparsity and smoothness of the effect. To incorporate spatial dependence structure of the predictors, Reiss and Ogden (2010) extended the functional principal component regression originally proposed for one dimensional functional covariates to high dimensional predictors. They modeled the coefficient function by using B-spline functions and considered common smoothing spline penalty which is not sensitive to sharp edges and jumps. Recently, Wang and Zhu (2015) proposed a new type of penalty - based on the total variation of the function - which yields piecewise smooth regression coefficients. While these approaches are computationally efficient, none of them can fully take into account the spatial dependence of the image predictor. In addition, in this framework it is not clear how to assess statistical significance.

To overcome some of these limitations, this problem has been also approached from

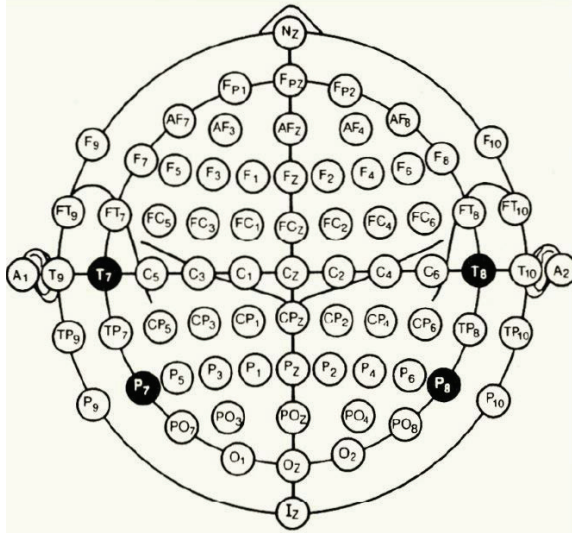
a Bayesian viewpoint. Goldsmith et al. (2014) proposed two latent spatial processes to model the sparsity and the smoothness of the regression coefficient: specifically an Ising prior was used for the binary indicator variable that controls whether a voxel image is predictive of the response or not (sparsity), and a conditional autoregressive Gaussian process for the non-zero regression coefficients to improve the model prediction (smoothness). The use of Ising prior for the binary indicator was first discussed in Smith and Fahrmeir (2007) in the context of high dimensional predictors and was also recently exploited by Li et al. (2015) who proposed it jointly with a Dirichlet process prior. To address the computational challenge of a non-closed form for the probability function, the latter work proposed an analytical approach to derive bounds for the hyperparameters. One of the characteristics of both Li et al. (2015) and Goldsmith et al. (2014) is that the sparsity and smoothness are controlled separately by two different spatial processes. As a result, the transition from zero-areas to non-zero neighboring areas in the regression coefficient may be very abrupt. This does not seem realistic for entire brain regions, where it is expected to see a gradual effect in contain brain areas on the response.

We propose a novel approach to spatial variable selection in the scalar-on-image regression by modeling the regression coefficients through a soft-thresholding transformation of latent Gaussian processes, to which we refer as soft-thresholded Gaussian processes. The soft-thresholding function is well known as the solution for the lasso estimate when the design matrix is orthonormal (Tibshirani 1996). The soft-thresholded Gaussian process leads to different model properties than the existent literature: in particular it ensures a gradual transition between the zero and non-zero effects of the neighboring locations. Theoretically, we can show that it provides a large support for the spatially varying coefficient function in the model that enjoys piecewise smoothness, sparsity and continuous properties. The idea is inspired from

Boehm Vock et al. (2014) who considered it as a regularization technique for spatial variable selection. This approach does not assign prior probability mass at zero for regression coefficients and it is not designed for the scalar-on-image regression. The use of the soft-thresholded Gaussian process has an attractive computational advantage over the competing methods, where the use of Ising prior makes it impossible to have a closed form probability distribution function making the computations challenging. In particular, we consider a low-rank spatial model for the latent process, which is important for the scalability of the method to large datasets. For theoretical results, in addition to the large support, we also can show that the soft-thresholded Gaussian process leads to the posterior consistency for both parameter estimation and variable selection for scalar-on-image regression. That is, the posterior distribution of the spatially varying coefficient function concentrates in a small neighborhood of the true value and the its sign is also consistent with the true value with probability one as the number of subjects goes to infinity. These two results only need a few mild regularity conditions; the conclusions hold even when the number of true predictors is larger than the sample size.

The proposed method is introduced for the case of single image predictor and Gaussian responses for simplicity. Nevertheless extensions to accommodate other type of covariates through a linear effect as well as generalized responses are straightforward. The methods are applied to the data from an electroencephalography (EEG) study of alcoholism (<http://kdd.ics.uci.edu/datasets/eeg/eeg.data.html>), where of interest was to study the relation between the alcoholism status and the electrical brain activity over time. The data have been previously described in Li et al. (2010) and Zhou and Li (2014) and consist of EEG signals received from 64 channel of electrodes located on subjects' scalp, corresponding to alcoholic subjects and healthy controls. The EEG signals are recorded for 256 seconds; leading to a high-dimensional predic-

Figure 1: The standard electrode position nomenclature for 10-10 system



tor. Previous literature that analyzed these data ignored the spatial locations of the electrodes on the scalp, and thus considered a two-dimensional predictor. In contrast, we recover the locations of the electrodes from the standard electrode position nomenclature described by Fig. 1 of <https://www.acns.org/pdf/guidelines/Guideline-5.pdf>, as shown in Fig. 1. We study the same scientific question by accounting for the space-temporal dependence of the predictor.

2 Model

2.1 Scalar-on-image regression

Let \mathbb{R}^d be a d -dimensional vector space of real values for any integer $d \geq 1$. Suppose there are n subjects in the dataset. For each subject i , we collect a scalar response variable, $Y_i \in \mathbb{R}^1$, a set of p_n spatially distributed imaging predictors, denoted $X_i = (X_{i,1}, \dots, X_{i,p_n})^T \in \mathbb{R}^{p_n}$ and other scalar covariates $W_i = (W_{i,1}, \dots, W_{i,q})^T \in \mathbb{R}^q$, where $X_{i,j}$ denotes the image intensity values measured at location s_j , for $j = 1, \dots, p_n$. Write $S = \{s_j\}_{j=1}^{p_n}$ which is an subset of a compact closed region $\mathcal{B} \subseteq \mathbb{R}^d$.

Let $N(\mu, \Sigma)$ be a normal distribution with mean μ and covariance Σ (or variance for one dimensional case). We consider the following scalar-on-image regression model: for $i = 1, \dots, n$,

$$\{Y_i \mid W_i, X_i, \alpha^v, \beta, \sigma^2, S\} \sim N \left\{ \sum_{k=1}^q \alpha_k W_{i,k} + p_n^{-1/2} \sum_{j=1}^{p_n} \beta(s_j) X_{i,j}, \sigma^2 \right\}, \quad (1)$$

where $\alpha^v = (\alpha_1, \dots, \alpha_q)^T$ is the coefficient for the scalar covariates W_i and $\beta(s)$ is a spatially varying coefficient function defined on \mathcal{B} for imaging predictor X_i . Assume that $\{W_i\}_{i=1}^n$ are fixed design covariates and S collects all fixed spatial locations. In practice, the normalizing scalar $p_n^{-1/2}$ can be absorbed into imaging predictors; its role is to rescale the total effects of massive imaging predictors such that they are bounded away from infinity with a large probability when p_n is very large. Scientifically, imaging predictors take values that measure the body tissue contrast or the neural activities at each spatial location and the number of imaging predictors, p_n is determined by the resolution of the image. Thus, the total effects of imaging predictors reflect the total amount of the intensity in the brain signals, which should not increase to infinity as the image resolution increases. In model (1), the response is taken to be Gaussian and only one type of imaging predictor is included, although extensions to non-Gaussian responses and multi-modality imaging predictor regression are straightforward.

2.2 Soft-thresholded Gaussian Processes

In order to capture the characteristics of imaging predictors and their effects on the response variable, the prior for the covariate function β should be sparse and spatial. That is, we assume that many locations have $\beta(s_j) = 0$; the sites with non-zero coefficients cluster spatially, and that the coefficients vary smoothly in clusters of non-zero coefficients. To encode these desired properties into the prior, we represent $\beta(s)$ as a transformation of a Gaussian process, $\beta(s) = g_\lambda\{\tilde{\beta}(s)\}$, where g_λ is the transformation

function dependent on parameter λ and $\tilde{\beta}(s)$ follows a Gaussian process prior. In this transkriging (Cressie 1993) or Gaussian copula (Nelsen 1999) model, the function g_λ determines the marginal distribution of $\beta(s)$, while the covariance of the latent $\tilde{\beta}(s)$ determines $\beta(s)$'s dependence structure.

Spatial dependence is determined by the prior for $\tilde{\beta}(s)$. We assume that $\tilde{\beta}(s)$ is a Gaussian process with zero-mean and stationary covariance function $\text{cov}\{\tilde{\beta}(s), \tilde{\beta}(s')\} = \kappa(s - s')$ for some covariance function κ . Although other transformations are possible (Boehm Vock et al. 2014), we select g_λ to be the soft-thresholding function to map $\tilde{\beta}(s)$ near zero to exact zero and thus give a sparse prior. Let

$$g_\lambda(x) = \begin{cases} 0 & |x| \leq \lambda \\ \text{sgn}(x)(|x| - \lambda) & |x| > \lambda \end{cases}, \quad (2)$$

where $\text{sgn}(x)$ is the sign of x , i.e. $\text{sgn}(x) = 1$ if $x > 0$ and $\text{sgn}(x) = -1$ if $x < 0$ and $\text{sgn}(0) = 0$. The thresholding parameter $\lambda > 0$ determines the degree of sparsity. This soft-thresholded Gaussian process prior is denoted $\beta \sim \text{STGP}(\lambda, \kappa)$.

3 Theoretical Properties

In this section, we examine the theoretical properties of soft thresholded Gaussian processes as prior models for scalar-on-image regression. We first introduce the formal definition for the class of the true spatially varying coefficients in the model that can well characterize the effects of the imaging predictors on the response variable. In light of good properties of the soft thresholding function (Lemmas 1 – 2), we show that the soft thresholded Gaussian processes have large support for the true spatially varying coefficient functions in the class we define (Theorem 1). Then we can verify the prior positivity of neighborhoods (Lemma 3) and construct uniform consistent tests (Lemma 5) which are needed to define a sieve of spatially varying coefficient functions and find the upper bound of the tail probability (Lemmas A.6–A.4), and verify that the model is identifiable (Lemmas A.7–A.10) under certain regularity

conditions. Thus, following the theory developed by Choudhuri et al. (2004), we show the posterior consistency (Theorem 2). Given the smoothness and sparsity of the soft-thresholded Gaussian process, we can further show the posterior sign consistency for the sparse spatially varying coefficient function (Theorem 3), indicating the posterior spatial variable selection consistency.

3.1 Notations and Definitions

We start with additional notations for the theoretical development and the formal definitions of the class of spatially varying coefficient functions under consideration. We assume that all the random variables and stochastic processes that we introduced in this article are defined in the same probability space, denoted $(\Omega, \mathcal{F}, \Pi)$. Recall that \mathbb{R}^d represents the d -dimensional vector space of real values. Let $\mathbb{Z}_+^d = \{0, 1, \dots\}^d \subset \mathbb{R}^d$ represent the d -dimensional vector space of non-negative integers. For any vector $\mathbf{v} = (v_1, \dots, v_d)^\top \in \mathbb{R}^d$, let $\|\mathbf{v}\|_p = (\sum_{l=1}^d |v_l|^p)^{1/p}$ be the L^p norm for vector \mathbf{v} for any $p \geq 1$, and $\|\mathbf{v}\|_\infty = \max_{l=1}^d |v_l|$ be the supremum norm. For any $x \in \mathbb{R}$, let $\lceil x \rceil$ be the smallest integer larger than x and $\lfloor x \rfloor$ be the largest integer smaller than x . Define the event indicator $I(\mathcal{A}) \in \{0, 1\}$ with $I[\mathcal{A}] = 1$ if event \mathcal{A} occurs, $I[\mathcal{A}] = 0$ otherwise. For any $\mathbf{z} = (z_1, \dots, z_d)^\top \in \mathbb{Z}_+^d$, define $\mathbf{z}! = \prod_{l=1}^d \prod_{k=1}^{z_l} k$ and define $\mathbf{v}^{\mathbf{z}} = \prod_{l=1}^d v_l^{z_l}$.

Definition 1. Let $f(\mathbf{s})$ be defined in the set $\mathcal{B} \subseteq \mathbb{R}^d$ for $\mathbf{s} = (s_1, \dots, s_d)$, and let m be a non-negative integer. We say $f(\mathbf{s})$ is a differentiable function of order m , if $f(\mathbf{s})$ has partial derivatives

$$D^{\bar{\tau}} f(\mathbf{s}) = \frac{\partial^{|\bar{\tau}|} f}{s_1^{\tau_1} \dots s_d^{\tau_d}}(\mathbf{s}) = \sum_{\|\bar{\eta}\|_1 + \|\bar{\tau}\|_1 \leq m} \frac{D^{\bar{\tau} + \bar{\eta}} f(\mathbf{t})}{\bar{\eta}!} (\mathbf{s} - \mathbf{t})^{\bar{\eta}} + R_m(\mathbf{s}, \mathbf{t}),$$

where $\bar{\tau} = (\tau_1, \dots, \tau_d)^\top \in \mathbb{Z}_+^d$, $\bar{\eta} \in \mathbb{Z}_+^d$ and $\mathbf{t} \in \mathbb{R}^d$.

Denote by $\mathcal{C}^m(\mathcal{B})$ a set of differentiable functions of order m defined on \mathcal{B} . For any $f \in \mathcal{C}^m(\mathcal{B})$, define the L^p norm $\|f\|_p = (\int_{\mathcal{B}} |f(\mathbf{s})|^p ds)^{1/p}$ for any $p \geq 1$ and the

supremum norm is $\|f\|_\infty = \sup_{s \in \mathcal{B}} |f(s)|$. The remainder $R_m(s, t)$ has the following property. Given any point s_0 of \mathcal{B} and any $\epsilon > 0$, there is a $\delta > 0$ such that if s and t are any two points of \mathcal{B} with $\|s - s_0\|_1 < \delta$ and $\|t - s_0\|_1 < \delta$, then $|R_m(s, t)| \leq \|s - t\|_1^{m - \|\bar{\tau}\|_1} \epsilon$. If $\|D^{\bar{\tau}} f\|_\infty \leq M < \infty$, then $|R_m(s, t)| \leq (M \|s - t\|_1^{m+1}) / (m+1)!$.

Definition 2. Denote by $\bar{\mathcal{R}}$ and $\partial\mathcal{R}$ the closure and the boundary of any set $\mathcal{R} \subseteq \mathcal{B}$. Define a collection of functions $\beta(s)$ that satisfy the following properties. That is, there exist two disjoint non-empty open sets \mathcal{R}_{-1} and \mathcal{R}_1 with $\bar{\mathcal{R}}_1 \cap \bar{\mathcal{R}}_{-1} = \emptyset$ such that

(2.1) *Piecewise Smoothness:* $\beta(s)$ is smooth over $\bar{\mathcal{R}}_{-1} \cup \bar{\mathcal{R}}_1$, i.e.

$$\beta(s)I[s \in \bar{\mathcal{R}}_{-1} \cup \bar{\mathcal{R}}_1] \in \mathcal{C}^\rho(\bar{\mathcal{R}}_{-1} \cup \bar{\mathcal{R}}_1), \text{ with } \rho = \lceil d/2 \rceil.$$

(2.2) *Sparsity:* $\beta(s) = 0$ for $s \in \mathcal{R}_0$, $\beta(s) > 0$ for $s \in \mathcal{R}_1$ and $\beta(s) < 0$ for $s \in \mathcal{R}_{-1}$, where $\mathcal{R}_0 = \mathcal{B} - (\mathcal{R}_{-1} \cup \mathcal{R}_1)$ and $\mathcal{R}_0 - (\partial\mathcal{R}_1 \cup \partial\mathcal{R}_{-1}) \neq \emptyset$.

(2.3) *Continuity:* $\beta(s)$ is continuous over \mathcal{B} . That is,

$$\lim_{s \rightarrow s_0} \beta(s) = \beta(s_0), \quad \text{for any } s_0 \in \mathcal{B}.$$

Define Θ as a collection of all spatially varying coefficient functions that satisfy with conditions (2.1) – (2.3) in Definition 2.

3.2 Conditions for Theoretical Results

In this section, we list all the conditions that are needed to facilitate the theoretical results, although they may not be the weakest conditions.

Condition 1. There exists $M_0 > 0$, $M_1 > 0$, $N \geq 1$, and some v_0 , $d/(2\rho) < v_0 < 1$ and $\rho = \lceil d/2 \rceil$ such that for all $n > N$, $M_0 n^d \leq p_n \leq M_1 n^{2\rho v_0}$.

This condition implies that the number of imaging predictors p_n should be of polynomial order of sample size. The lower bound indicates that p_n needs to be sufficiently large such that the posterior distribution of the spatially varying coefficient function concentrates around the true value.

Condition 2. *The true spatially varying coefficient function in model (1) enjoys the piecewise smoothness, sparsity and continuity properties, in short, $\beta_0 \in \Theta$.*

The next two conditions summarize constraints on the spatial locations and the distribution of the imaging predictors.

Condition 3. *For the observed spatial locations $S = \{s_j\}_{j=1}^{p_n}$ in region \mathcal{B} , there exists a set of sub-regions $\{\mathcal{B}_j\}_{j=1}^{p_n}$ satisfying the following conditions:*

(3.1) *They form a partition of \mathcal{B} , i.e. $\mathcal{B} = \bigcup_{j=1}^{p_n} \mathcal{B}_j$ with $\mathcal{B}_j \cap \mathcal{B}_{j'} = \emptyset$.*

(3.2) *For each $j = 1, \dots, p_n$, $s_j \in \mathcal{B}_j$ and $V(\mathcal{B}_j) \leq \zeta(\mathcal{B}_j) < \infty$, where $V(\bullet)$ is the Lebesgue measure and*

$$\zeta(\mathcal{B}) = \sup_{\mathbf{t}, \mathbf{t}' \in \mathcal{B}} \left[\max_k |t_k - t'_k| \right]^d, \quad \text{with } \mathbf{t} = (t_1, \dots, t_d)^T \text{ and } \mathbf{t}' = (t'_1, \dots, t'_d)^T.$$

(3.3) *There exists a constant $0 < K < V(\mathcal{B})$ such that $\max_j \zeta(\mathcal{B}_j) < 1/(Kp_n)$ as $n \rightarrow \infty$.*

When \mathcal{B} is a hypercube in \mathcal{R}^d , e.g. $\mathcal{B} = [0, 1]^d$, there exists a set of $\{\mathcal{B}_j\}_{j=1}^{p_n}$ that equally partitions \mathcal{B} . Then $V(\mathcal{B}_j) = \zeta(\mathcal{B}_j) = p_n^{-1}$.

Condition 4. *The covariate variables $\{X_{i,1}, \dots, X_{i,p_n}\}_{i=1}^n$ are independent realizations of a stochastic process $X(\mathbf{s})$ at spatial locations s_1, \dots, s_{p_n} . The stochastic process $X(\mathbf{s})$ satisfies*

(4.1) *$E[X(\mathbf{s})] = 0$ for all $\mathbf{s} \in \mathcal{B}$.*

(4.2) For all $n > 1$, let $\Sigma_n = (\sigma_{j,j'})_{1 \leq j, j' \leq p_n}$ where $\sigma_{j,j'} = E[X(s_j)X(s_{j'})]$. Let $\rho_{\min}(A)$ and $\rho_{\max}(A)$ be the smallest eigenvalue and the largest eigenvalue of a matrix A , respectively. Then there exist c_{\min} and c_{\max} with $0 < c_{\min} \leq 1$ and $0 < c_{\max} < \infty$ such that for $n > 1$,

$$\rho_{\min}(\Sigma_n) > c_{\min} \text{ and } \rho_{\max}(\Sigma_n) < c_{\max}.$$

(4.3) For any $\epsilon > 0$ and $M < \infty$, there exists $\delta > 0$ such that for any $a_1, \dots, a_{p_n} \in \mathbb{R}$ with $|a_j| < M$ for all j , if there exists N , for all n , $p^{-1} \sum_{j=1}^{p_n} |a_j| > \epsilon$, then

$$\Pi \left[p_n^{-1/2} \left| \sum_{j=1}^{p_n} a_j X(s_j) \right| > \delta \right] > \delta.$$

Condition 4 includes assumptions on the mean of $X(s)$ and on the range of eigenvalues of the covariance matrix Σ_n for covariate variables. If Gaussian process $X(s)$ on $[0, 1]^d$ has zero mean and $E[X(s_j)X(s_{j'})] = \rho_0 \exp(-p_n \|s_j - s_{j'}\|_1)$, $0 < \rho_0 < 1$, if $j \neq j'$ and $E[X(s_j)^2] = 1$, where $\{s_j\}_{j=1}^{p_n}$ are chosen as the centers of the equal space partitions of \mathcal{B} , then condition (4.2) holds. Furthermore, condition (4.3) also holds. Specifically, for any $\epsilon > 0$, taking $\delta = c_{\min}^{1/2} \epsilon \exp(-\epsilon)$, for any a_1, \dots, a_{p_n} , let $\xi = p_n^{-1/2} \sum_{j=1}^{p_n} a_j X(s_j) \sim N(0, \kappa^2)$, By Condition (4.2),

$$\kappa^2 = \frac{1}{p_n} \sum_{j,j'} a_j \sigma_{j,j'} a_{j'} \geq \frac{1}{p_n} \sum_{j=1}^{p_n} a_j^2 \rho_{\min}(\Sigma_n) > c_{\min} \frac{1}{p_n} \sum_{j=1}^{p_n} a_j^2.$$

There exists N , such that for all $n > N$, $\left(p_n^{-1} \sum_{j=1}^{p_n} a_j^2 \right)^{1/2} \geq p_n^{-1} \sum_{j=1}^{p_n} |a_j| > \epsilon$. Thus, $\kappa^2 > c_{\min} \epsilon^2$. Furthermore,

$$\Pi[|\xi| > \delta] = 2\Phi(-\kappa^{-1}\delta) > 2\Phi\left(-c_{\min}^{-1/2} \epsilon^{-1} \delta\right) = 2\Phi\{-\exp(-\epsilon)\} > \epsilon \exp(-\epsilon) > \delta.$$

To ensure the large support property, we need the following condition on the kernel function of the Gaussian process. This condition also has been used previously by Ghosal and Roy (2006).

Condition 5. For every fixed $s \in \mathcal{B}$, the covariance kernel $\kappa(s, \cdot)$ has continuous partial derivatives up to order $2\rho + 2$.

3.3 Large Support

One of the desired properties for the Bayesian nonparametric model is to have prior support over a large class of functions. In this section, we show that the support of the soft-thresholded Gaussian process is large for any spatially varying coefficient function of our interests in the scalar-on-image regression. We begin with two appealing properties of the soft-thresholding function in the following two lemmas.

Lemma 1. The soft-thresholding function $g_\lambda(x)$ is Lipschitz continuous for any $\lambda > 0$, that is, for all $x_1, x_2 \in \mathbb{R}$, $|g_\lambda(x_1) - g_\lambda(x_2)| \leq |x_1 - x_2|$.

Lemma 2. For any function $\beta_0 \in \Theta$, there exists a threshold parameter λ_0 and a smooth function $\tilde{\beta}_0(s) \in \mathcal{C}^\rho(\mathcal{B})$ such that $\beta_0(s) = g_{\lambda_0}\{\tilde{\beta}_0(s)\}$.

The proof of lemma 1 is straightforward by verifying the definition. The proof of lemma 2 is not trivial, it requires a detailed construction on the smooth function $\tilde{\beta}_0(s)$. Please refer to the Appendix for details.

Theorem 1. (Large Support) For a function $\beta_0 \in \Theta$, there exists a thresholding parameter λ_0 , such that the soft thresholded Gaussian process prior $\beta \sim \mathcal{STGP}(\lambda_0, \kappa)$ satisfies

$$\Pi(\|\beta - \beta_0\|_\infty < \varepsilon) > 0, \quad \text{for all } \varepsilon > 0.$$

Proof. By Lemma 2, there exists a thresholding parameter λ_0 and a smooth function $\tilde{\beta}_0(s)$ such that $\beta_0(s) = g_{\lambda_0}[\tilde{\beta}_0(s)]$. Since $\beta \sim \mathcal{STGP}(\lambda_0, \kappa)$, we have $\beta(s) = g_{\lambda_0}[\tilde{\beta}(s)]$ with $\tilde{\beta}(s) \sim \mathcal{GP}(0, \kappa)$, By Lemma 1 and Theorem 4 of (Ghosal and Roy 2006)

$$\begin{aligned} \Pi\left(\sup_{s \in \mathcal{B}} |\beta(s) - \beta_0(s)| < \varepsilon\right) &= \Pi\left(\sup_{s \in \mathcal{B}} |g_{\lambda_0}(\tilde{\beta}(s)) - g_{\lambda_0}(\tilde{\beta}_0(s))| < \varepsilon\right) \\ &\geq \Pi\left(\sup_{s \in \mathcal{B}} |\tilde{\beta}(s) - \tilde{\beta}_0(s)| < \varepsilon\right) > 0. \end{aligned}$$

□

Theorem 1 implies that there is always a positive probability that the soft-thresholded Gaussian process concentrates in an arbitrarily small neighborhood of any spatially varying coefficient function that has piecewise smoothness, sparsity and continuity properties.

3.4 Posterior Consistency

For $i = 1, \dots, n$, given the image predictor X_i on a set of spatial locations S and other covariates W_i , suppose the response Y_i is generated from the scalar-on-image regression model (1) with parameters $\alpha_0^v \in \mathbb{R}^q$, $\sigma_0^2 > 0$ that are known and parameter of interest $\beta_0 \in \Theta$. The assumptions about α_0^v and σ_0^2 are for theoretical convenience; in practice it is straightforward to estimate from the data. We assign a soft-thresholded Gaussian process prior for the spatially varying coefficient function, i.e. $\beta \sim \mathcal{STGP}(\lambda_0, \kappa)$ for some known $\lambda_0 > 0$ and covariance kernel κ . In light of the large support by Theorem 1, the following lemma shows the positivity of prior neighborhoods:

Lemma 3. (*Positivity of prior neighborhoods*) Denote by $\pi_{n,i}(\bullet; \beta)$ the density function of $Z_{n,i} = (Y_i, X_i)$ in model (1) and suppose condition (4) holds for X_i . Define

$$\begin{aligned} \Lambda_{n,i}(\bullet; \beta_0, \beta) &= \log \pi_{n,i}(\bullet; \beta) - \log \pi_{n,i}(\bullet; \beta_0), \\ K_{n,i}(\beta_0, \beta) &= E_{\beta_0} \{ \Lambda_{n,i}(Z_{n,i}; \beta_0, \beta) \}, \text{ and} \\ V_{n,i}(\beta_0, \beta) &= \text{var}_{\beta_0} \{ \Lambda_{n,i}(Z_{n,i}; \beta_0, \beta) \}. \end{aligned}$$

There exists a set B with $\Pi(B) > 0$ such that, for any $\epsilon > 0$,

$$\liminf_{n \rightarrow \infty} \Pi \left[\left\{ \beta \in B, \frac{1}{n} \sum_{i=1}^n K_{n,i}(\beta_0, \beta) < \epsilon \right\} \right] > 0, \quad \text{and} \quad \frac{1}{n^2} \sum_{i=1}^n V_{n,i}(\beta_0, \beta) \rightarrow 0, \text{ for all } \beta \in B.$$

We construct sieves for the spatially varying coefficient functions in Θ as

$$\Theta_n = \left\{ \beta \in \Theta : \|\beta\|_\infty \leq p_n^{1/(2d)}, \sup_{s \in \mathcal{R}_1 \cup \mathcal{R}_{-1}} |D^{\bar{\tau}} \beta(s)| \leq p_n^{1/(2d)}, 1 \leq \|\bar{\tau}\|_1 \leq \rho \right\},$$

and by Lemmas A.6 – A.10 in the appendix, we can find the upper bound of the tail probability and construct uniform consistent tests in the following lemmas:

Lemma 4. *Suppose $\beta(s) \sim \mathcal{STGP}(\lambda_0, \kappa)$ with $\lambda_0 > 0$ and the kernel function κ satisfies condition 5, then there exist constants K and b such that for all $n \geq 1$,*

$$\Pi(\Theta_n^C) \leq K \exp(-bp_n^{1/d}).$$

Lemma 5. *(Uniform consistent tests) For any $\epsilon > 0$ and $v_0/2 < v < 1/2$, there exist N, C_0, C_1 and C_2 such that for all $n > N$ and all $\beta \in \Theta_n$, if $\|\beta - \beta_0\|_1 > \epsilon$, a test function Ψ_n can be constructed such that*

$$E_{\beta_0}(\Psi_n) \leq C_0 \exp(-C_2 n^{2v}), \text{ and } E_\beta(1 - \Psi_n) \leq C_0 \exp(-C_1 n).$$

Proofs of Lemmas 3–5 are provided in the online supplementary materials. These lemmas verify three important conditions for proving posterior consistency in the scalar-on-image regression based on Theorem A.1 by Choudhuri et al. (2004). Thus, we have the following theorem:

Theorem 2. *(Posterior Consistency) Write data $D_n = [\{Y_i\}_{i=1}^n, \{X_i\}_{i=1}^n, \{W_i\}_{i=1}^n]$. If Conditions 1 – 5 hold, then for any $\epsilon > 0$,*

$$\Pi[\beta \in \Theta : \|\beta - \beta_0\|_1 < \epsilon \mid D_n] \rightarrow 1,$$

as $n \rightarrow \infty$ in $P_{\beta_0}^n$ probability, where $P_{\beta_0}^n$ denotes the actual distribution of data D_n .

Theorem 2 implies that the soft-thresholded Gaussian process prior can ensure that the posterior distribution of the spatially varying coefficient function concentrates in an arbitrarily small neighborhood of the true value, when both the number of

subjects and number of spatial locations are sufficiently large. Given that the true function of interest is piecewise smooth, sparse and continuous, the soft-threshold Gaussian process prior can further ensure that the posterior probability of the sign of the spatially varying coefficient function being correct converges to one as the sample size goes to infinity. The result is formally stated in the following theorem.

Theorem 3. (*Posterior Sign Consistency*) *Suppose the model assumptions, prior settings and regularity conditions for Theorem 2 hold.*

$$\Pi [\text{sgn}\{\beta(s)\} = \text{sgn}\{\beta_0(s)\}, \text{ for all } s \in \mathcal{B} \mid \mathcal{D}_n] \rightarrow 1,$$

as $n \rightarrow \infty$ in $P_{\beta_0}^n$ probability.

This theorem establishes the spatial variable selection consistency. It does not require the number of true imaging predictors is finite or less than the sample size. This is different from most previous results, but it is reasonable in that the true spatially varying coefficient function is piecewise smooth and continuous and the soft-thresholded Gaussian process will borrow strength from neighboring locations to estimate the true imaging predictors. Please refer to the Appendix for the proofs of Theorems 2 and 3.

4 Posterior Computation

4.1 Model Representation and Prior Specifications

We turn now to the practical applicability of our proposed method. We select a low-rank spatial model to ensure that computation remains possible for applications with large datasets. We exploit the kernel convolution approximation of a spatial Gaussian process. As discussed in Higdon et al. (1999), any stationary Gaussian process $V(s)$ can be written $V(s) = \int K(s_j - t)w(t)dt$, where K is a kernel function and w is a

white-noise process with mean zero and variance σ_w^2 . This gives covariance function

$$\text{cov}(\mathbf{s}, \mathbf{s} + \mathbf{h}) = \kappa(\mathbf{h}) = \sigma_a^2 \int K(\mathbf{s} - \mathbf{t})K(\mathbf{s} + \mathbf{h} - \mathbf{t})d\mathbf{t},$$

which illustrates the connection between covariance κ and kernel K . This representation suggests the approximation for the latent Gaussian process

$$\tilde{\beta}(\mathbf{s}) = \sum_{l=1}^L K(\mathbf{s} - \mathbf{t}_l)a_l,$$

where $\mathbf{t}_1, \dots, \mathbf{t}_L \in \mathbb{R}^d$ are a grid of spatial knots covering \mathcal{B} , K is a local kernel function, and $a_l \sim N(0, \sigma_a^2)$ is the coefficient associated with knot l . We use tapered Gaussian kernels with bandwidth σ_h ,

$$K(h) = \exp \left[-\frac{h^2}{2\sigma_h^2} \right] I(h < 3\sigma_h),$$

so that $K(\|\mathbf{s} - \mathbf{t}_l\|) = 0$ for \mathbf{s} separated from \mathbf{t}_l by at least $3\sigma_h$. Taking $L < p$ knots and selecting compact kernels both lead to computational savings, as discussed in Section 4.2.

The compact kernels K control the local spatial structure and the prior for the coefficients $\mathbf{a} = (a_1, \dots, a_L)^T$ controls broad spatial structure. Following the work by Nychka et al. (2015) for geostatistical data, we assume that the knots $\mathbf{t}_1, \dots, \mathbf{t}_L$ are arranged on an $m_1 \times \dots \times m_d$ array, and use $l \sim k$ to denote that knots \mathbf{t}_l and \mathbf{t}_k are adjacent on this array. We then use a conditionally autoregressive prior (Gelfand et al. 2010) for the kernel coefficients. The conditional autoregressive prior is also defined locally, with full conditional distribution

$$a_l | a_k, k \neq l \sim N \left(\frac{\vartheta}{n_l} \sum_{k \sim l} a_k, \frac{\sigma_a^2}{n_l} \right), \quad (3)$$

where n_l is the number of knots adjacent to knot l , $\vartheta \in (0, 1)$ determines the strength of spatial dependence, and σ_a^2 determines the variance. These full conditional distributions correspond to the joint distribution $\mathbf{a} \sim N[0, \sigma_a^2(\mathbf{M} - \vartheta\mathbf{A})^{-1}]$, where \mathbf{M} is

diagonal with diagonal elements $\{n_1, \dots, n_L\}$ and A is the adjacency matrix with (k, l) element equal 1 if $k \sim l$ and zero otherwise (including zeros on the diagonal).

Write $\tilde{\beta}^v = \{\tilde{\beta}(s_1), \dots, \tilde{\beta}(s_p)\}^T$. Denote by K the $p \times L$ kernel matrix with (j, l) element $K(\|s_j - t_l\|_2)$, the prior for $\tilde{\beta}^v$ is given by $\tilde{\beta}^v \sim N\{0, \sigma_a^2 K(M - \vartheta A)^{-1} K^T\}$. In this case, the $\tilde{\beta}(s_j)$ do not have the equal variance, which may not generally be desirable. Non-constant variance arises because the kernel knots t_j may be unequally distributed, and because the conditional autoregressive model is non-stationary in that the variances of the a_l are unequal.

To stabilize the prior variance, define $\tilde{K}_{j,l} = K(\|s_j - t_l\|_2)/w_j$ and \tilde{K} as the corresponding $p \times L$ matrix of standardized kernel coefficients, where w_j are constants chosen so that the prior variance for each β_j is equal. We take w_j to be the j -th diagonal element of $\text{cov}(\tilde{\beta}^v) = K(M - \vartheta A)^{-1} K^T$, hence the kernel functions now depend on ϑ . By pulling the prior standard deviation σ_a out of the thresholding transformation, write $\beta^v = \{\beta(s_1), \dots, \beta(s_p)\}^T$, we have an equivalent model representation of model (1) as

$$Y_i \sim N[W_i^T \alpha^v + p_n^{-1/2} X_i^T \beta^v, \sigma^2], \text{ with } \beta(s_j) = \sigma_a g_\lambda\{\tilde{\beta}(s_j)\}, \quad (4)$$

where $\tilde{\beta}^v \sim N\{0, \tilde{K}(M - \vartheta A)^{-1} \tilde{K}^T\}$. After standardization the prior variance of each $\tilde{\beta}(s_j)$ is one, and therefore the prior probability that $\tilde{\beta}(s_j)$ is nonzero is $2\Phi(-\lambda)$ for all j , where $\Phi(\bullet)$ denotes the cumulative distribution function of standard normal distribution. This endows each parameter with a distinct interpretation: σ_a controls the scale of the non-zero coefficients; λ controls the prior degree of sparsity; and ϑ controls spatial dependence.

In practice, we normalize the response and covariates, and then select priors $\alpha^v \sim N(0, 10^2 I_q)$, $\sigma^2 \sim \text{InvGamma}(0.1, 0.1)$, $\sigma_a \sim \text{HalfNormal}(0, 1)$, $\vartheta \sim \text{Beta}(10, 1)$, and $\lambda \sim \text{Uniform}(\lambda_l, \lambda_u)$. Following Banerjee et al. (2004), we use a beta prior for ϑ with mean near one because only values near one provide appreciable spatial dependence.

In many of the cases considered in the simulation studies, the sparsity parameter λ cannot be fully identified. To improve numerical stability, we suggest an informative data-driven prior. We first fit the non-sparse model with $\lambda = 0$ and record the proportion of the $\beta(s_j)$ with posterior 95% credible interval that exclude zero, denoted u . The prior for λ then restricts the prior proportion of non-zeros to be within 0.05 of u , i.e., $\lambda_l = -\Phi^{-1}[(u + 0.05)/2]$ and $\lambda_u = -\Phi^{-1}[(u - 0.05)/2]$.

4.2 Markov chain Monte Carlo Algorithm

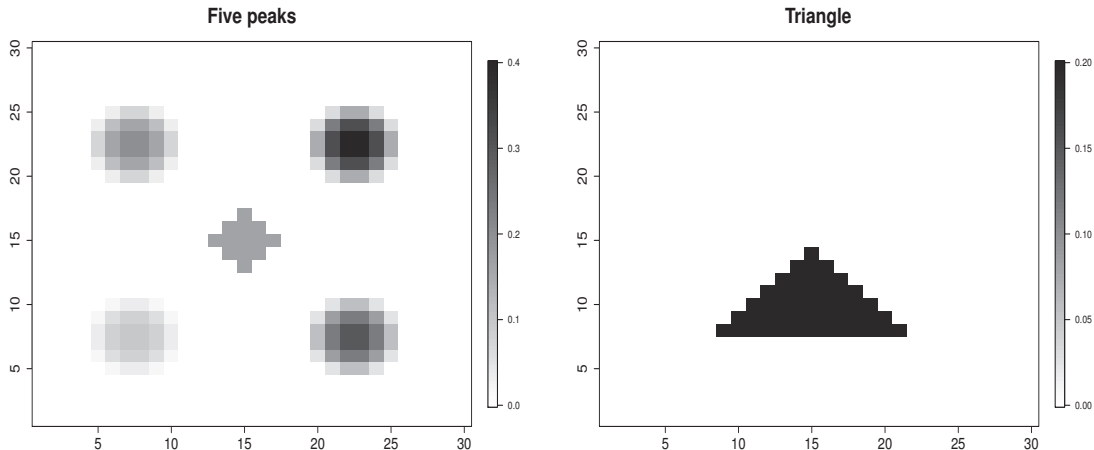
We sample from the posterior distribution using Metropolis-Hastings within Gibbs sampling. The parameters α^v , σ^2 , and σ_a^2 have conjugate full conditional distributions and are updated using Gibbs sampling. The spatial dependence parameter ϑ is sampled using Metropolis-Hastings sampling using a beta candidate distribution with the current value as mean and standard deviation tuned to give acceptance around 0.4. The threshold λ is updated using Metropolis sampling with random-walk Gaussian candidate distribution with standard deviation tuned to have acceptance probability around 0.4. The Metropolis update for a_l uses the prior full conditional distribution in (3) as the candidate distribution which gives high acceptance rate and thus good mixing without tuning.

5 Simulation study

5.1 Data generation

In this section we conduct a simulation study to compare the proposed methods with other popular methods for scalar-on-image regression. For each simulated observation, we generate a two-dimensional image X_i on the $m \times m$ grid $\{1, 2, \dots, m\}^2$ with $m = 30$. The covariates are generated following two covariance structures: exponential (“Exp”) and with shared structure (“SS”) with the signal, β^v . The exponential covariates are

Figure 2: True β^v images used in the simulation study.



Gaussian with mean $E(X_{ij}) = 0$ and $\text{cov}(X_{i,j}, X_{i,l}) = \exp(-d_{j,l}/\vartheta_X)$, where $d_{j,l}$ is the distance between locations j and l and ϑ_X controls the range of spatial dependence. The covariates generated with shared structure with β^v are $X_i = \tilde{X}_i/2 + e_i\beta^v$, where \tilde{X}_i is Gaussian with exponential covariance with $\vartheta_X = 3$ and $e_i \sim N(0, v^2)$; this is denoted as “SS(v)”. The response is then generated as $Y_i \sim N(X_i^T\beta^v, \sigma^2)$. Both X_i and Y_i are independent for $i = 1, \dots, n$. We consider two true β^v images (“Five peaks” and “Triangle”, plotted in Figure 2), sample sizes $n \in \{100, 250\}$, spatial correlation $\vartheta_X \in \{3, 6\}$, and error standard deviation $\sigma \in \{2, 5\}$. For all combinations of these parameters considered we generate $S = 100$ datasets.

5.2 Methods

We fit our model with a $m/2 \times m/2$ equally-spaced grid of knots covering $[1, m] \times [1, m]$ with bandwidth σ_h set to the minimum distance between knots. We fit the model both with $\lambda > 0$ and thus sparsity (“STGP”) and with $\lambda = 0$ and thus no sparsity (“GP”). For both models, we run the proposed Markov chain Monte Carlo algorithm

5,000 iterations with 1,000 burn-in, and compute the posterior mean of β^v . For the sparse model, we compute the posterior probability of a nonzero $\beta(s)$.

We compare our method with the lasso (Tibshirani 1996) and fused lasso (Tibshirani et al. 2005, Tibshirani and Taylor 2011) penalized regression estimates

$$\begin{aligned}\hat{\beta}_L^v &= \operatorname{argmin}_{\beta^v} \left\{ (Y - X\beta^v)^T(Y - X\beta^v) + \tilde{\lambda} \sum_j |\beta(s_j)| \right\}, \\ \hat{\beta}_{FL}^v &= \operatorname{argmin}_{\beta^v} \left\{ (Y - X\beta^v)^T(Y - X\beta^v) + \tilde{\lambda} \sum_{j \sim k} |\beta(s_j) - \beta(s_k)| + \tilde{\gamma} \tilde{\lambda} \sum_j |\beta(s_j)| \right\}.\end{aligned}\tag{5}$$

The lasso estimate $\hat{\beta}_L^v$ is computed using the `lars` package (Hastie and Efron 2013) in `R` (R Core Team 2013) and the tuning parameter $\tilde{\lambda}$ is selected using the Bayesian information criteria. The fused lasso estimate $\hat{\beta}_{FL}^v$ is computed using the `genlasso` package (Arnold and Tibshirani 2014) in `R` and the tuning parameters $\tilde{\gamma}$ and $\tilde{\lambda}$ are selected using the Bayesian information criteria. Due to computational considerations, we search only over $\tilde{\gamma} \in \{1/5, 1, 5\}$.

We also compare with a functional principle components analysis approach (“FPCA”). We smooth each image using the technique of Xiao et al. (2013) implemented in the `fbps` function in `R`’s `refund` package (Crainiceanu et al. 2014), compute the eigen decomposition of the sample covariance of the smoothed images, and then perform principal components regression using the lasso penalty tuned via the Bayesian information criteria. We use the leading eigenvectors that explain 90% of the variation in the sample images.

Finally, we compare with the Bayesian spatial model of Goldsmith et al. (2014) (“Ising”). Goldsmith et al. (2014) use the model $\beta(s_j) = \tilde{\alpha}_j \theta_j$, where $\tilde{\alpha}_j \in \{0, 1\}$ is the binary indicator that location j is included in the model, and $\theta_j \in \mathbb{R}$ is the regression coefficient given that the location is included. Both the $\tilde{\alpha}_j$ and θ_j have spatial priors; the continuous components θ_j follow a conditional autoregressive prior, and the binary components α_j follow an Ising (autologistic) prior (Gelfand et al. 2010)

with full conditional distributions

$$\text{logit}\{\Pi(\tilde{\alpha}_j = 1|\tilde{\alpha}_l, l \neq j)\} = a + b \sum_{l \sim j} \tilde{\alpha}_l. \quad (6)$$

Estimating a and b is challenging because of the complexity of the Ising model (Møller et al. 2006), therefore Goldsmith et al. (2014) recommend selecting a and b using cross validation over $a \in (-4, 0)$ and $b \in (0, 2)$. Due to computational limitations we select values in the middle of these intervals and set $a = -2$ and $b = 1$. Similar to our approach, 5,000 Markov chain Monte Carlo samples are simulated for the Ising model, and the first 1,000 are discarded as burn-in, and the posterior mean of $\beta(\mathbf{s})$ and the posterior probability of a nonzero $\beta(\mathbf{s})$ are computed.

5.3 Results

Table 1 gives the mean squared error for β^v estimation (averaged over location), type I error and power for detect non-zero signals along with computing time. The soft-thresholded Gaussian process (STGP) model gives the smallest mean squared error when the covariate has exponential correlation. Compared to the Gaussian process (GP) model, adding thresholding reduces mean squared error by roughly 50% in many cases. As expected the functional principal component analysis (FPCA) methods gives the smallest mean squared error in final two scenarios where the covariates are generated to have a similar spatial pattern as the true signal. Even in this case, the proposed method outperforms the other methods that do not exploit this shared structure. For variable selection results, we only compare the proposed method with Fused lasso and the Ising model for a fair comparison, because Lasso does not incorporate spatial locations and other methods do not perform variable selection directly. The results show that Fused lasso has much larger Type I errors in all cases and the Ising model has a very small power to detect the signal in each case. It is clear that the proposed method is much better than Fused lasso and the Ising

model for variable selection accuracy. For the computing time, the proposed method is comparable to Fused lasso and faster than the Ising model.

6 Analysis of EEG data

Our motivating application is the study of the relationship between the electrical brain activity as measured through multi channel electroencephalographic (EEG) signals and genetic predisposition to alcoholism. EEG is a medical imaging technique that records the electrical activity in the brain by measuring the current flows produced when the neurons are activated. The study comprises a total of 122 subjects - 77 alcoholic subjects and 45 non-alcoholic controls. For each subject 64 electrodes were placed on their scalp and EEG was recorded from each electrode at a frequency of 256Hz. The electrode positions were located at standard sites (standard electrode position nomenclature; American Electroencephalographic Association (1991)). The subjects were presented with 120 trials under several settings involving one stimulus or two stimuli. We consider the multichannel average EEG across the 120 trials corresponding to a single stimulus. The dataset is publicly available at the University of California at Irvine Knowledge Discovery of Datasets <https://kdd.ics.uci.edu/databases/eeg/eeg.data.html>.

These data have been previously analyzed by Li et al. (2010), Hung and Wang (2013) and Zhou and Li (2014); however all the existing literature ignored the spatial location of the electrodes on the scalp and used instead their ID number, ranging from 1 to 64 which is assigned arbitrarily relative to the electrodes' position on the scalp. Our goal of the analysis is to detect the regions of brain which are most predictive of the alcoholism status; thus accounting for the actual position of the electrodes is a key component in our approach. In the absence of more sophisticated means to determine the electrodes' position on the scalp, we consider a lattice design and assign a two-

Table 1: Simulation study results. Methods are compared in terms of mean squared error for β^v (“MSE for β^v ”), Type I error (%) and Power (%) for feature detection along with CPU time (minutes). Data are generated for two true β_0^v (Fig. 2), covariance of the covariate X_i (exponential, “Exp(ϑ_X)”, and shared structure, “SS(ν)”), error standard deviation (σ), and sample size (n). Results are reported as the mean over the S simulated datasets.

(a) MSE (multiplied by 1000) for β

True β^v	cov (ϑ_X)	σ	n	Lasso	Fused lasso	FPCA	Ising	GP	STGP
Five peaks	Exp(3)	5	100	31.90	18.48	3.67	4.44	2.63	1.65
	Exp(6)	5	100	54.99	2.66	3.33	4.14	2.07	1.93
	Exp(3)	2	100	10.20	4.42	2.51	2.71	1.50	0.70
Triangle	Exp(3)	5	250	66.85	1.54	3.01	5.09	1.71	0.91
	Exp(3)	5	100	28.31	18.08	1.83	2.75	1.80	0.82
	Exp(6)	5	100	51.90	4.32	1.63	2.64	1.76	0.88
Triangle	Exp(3)	2	100	7.10	3.74	1.26	1.35	1.01	0.55
	Exp(3)	5	250	65.12	0.69	1.50	3.33	1.19	0.68
	SS(2)	5	100	105.80	70.65	0.98	2.77	3.28	1.40
	SS(4)	5	100	106.62	71.23	0.34	3.18	3.39	1.81

(b) Type I error (%)

cov	True β^v	n	Fused lasso	Ising	STGP
Exp	Five peaks	100	18.73	0.09	3.61
		250	25.88	0.17	5.62
	Triangle	100	19.63	0.06	3.09
		250	11.88	0.14	4.45
SS	Five peaks	100	19.58	0.00	0.39
		250	15.57	0.03	0.71
	Triangle	100	20.18	0.00	1.36
		250	1.38	0.03	2.14

(c) Power (%)

True β^v	cov	n	Fused lasso	Ising	STGP
Exp	Five peaks	100	35.21	4.41	44.78
		250	76.45	9.76	71.77
	Triangle	100	49.84	7.71	89.22
		250	93.90	15.84	96.63
SS	Five peaks	100	29.23	5.59	30.76
		250	49.01	7.52	48.74
	Triangle	100	37.86	7.02	75.53
		250	84.27	12.57	87.14

(d) Computing time (minutes)

True β	cov (ϑ_X)	σ	n	Lasso	Fused lasso	FPCA	Ising	GP	STGP
Five peaks	3	5	100	0.02	16.77	5.40	27.61	4.81	17.69

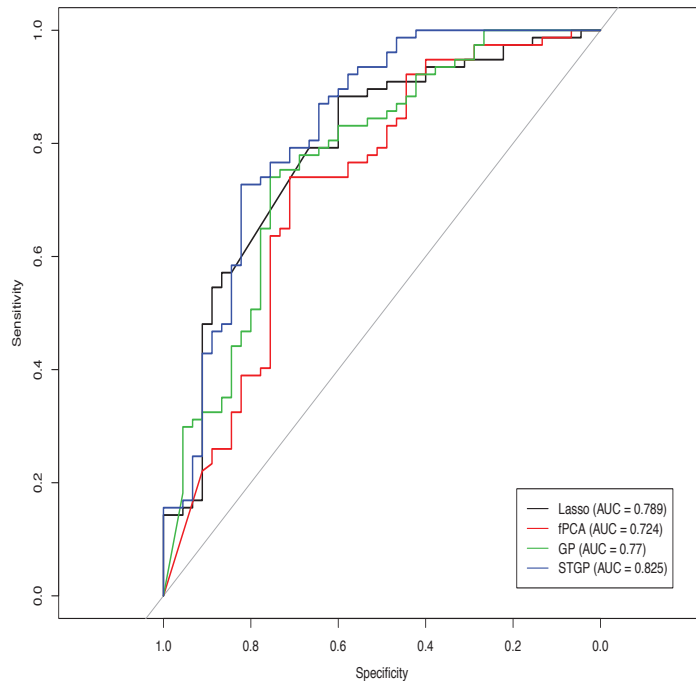
dimensional location to each electrode that matches closely the electrode’s standard position. Using the labels of the electrodes, we were able to identify only 60 of them. As a result our analysis will be based on the multichannel EEG from these 60 electrodes.

In accordance with the notation employed earlier, let Y_i be the alcoholism status indicator with $Y_i = 1$ if the i th subject is alcoholic and 0 otherwise. Furthermore, let $X_i = \{X_i(\mathbf{s}_j; t) : \mathbf{s}_j \in \mathbb{R}^2, j = 1, \dots, 60, t = 1, \dots, 256\}$ be the EEG image data for the i th subject which is indexed by a two-dimensional index accounting for the spatial location (on the matching lattice design), \mathbf{s}_j , and one-dimensional index for time, t .

We use a probit model to relate the alcoholism status and the multichannel EEG image: $Y_i | X_i, \beta \sim \text{Bernoulli}(p_i)$ and $\Phi^{-1}(p_i) = \sum_{j=1}^{60} \sum_{k=1}^{256} X_i(\mathbf{s}_j, t_k) \beta(\mathbf{s}_j, t_k)$. The spatially-temporally varying coefficient function β quantifies the effect of the image on the response over time and is modeled using the soft-thresholded Gaussian process on spatial and temporal domain. We select a 5×5 square grid of spatial knots and 64 temporal knots, for a total of 1,600 three-dimensional knots. We initially fit a conditional autoregressive model with a different dependence parameter ϑ for spatial and temporal neighbors (Reich et al. 2007), but found that the convergence was slow and that the estimates of both the spatial and temporal dependence were similar. Thus, we elected to use the same dependence parameter for all neighbors. Also, we consider an informative prior for the threshold $\lambda \sim \text{Uniform}(1.43, 1.96)$; intuitively this choice corresponds to an *a priori* inclusion probability between 5%-15%.

We evaluate the prediction performance of the proposed model. Figure 3 shows the receiving operating characteristic curve (ROC) using five-fold cross validation. The results are compared with the ones corresponding to the lasso, the functional principal component analysis and the Gaussian process approach (the soft-thresholding Gaussian process approach with thresholding parameter $\lambda = 0$). To facilitate com-

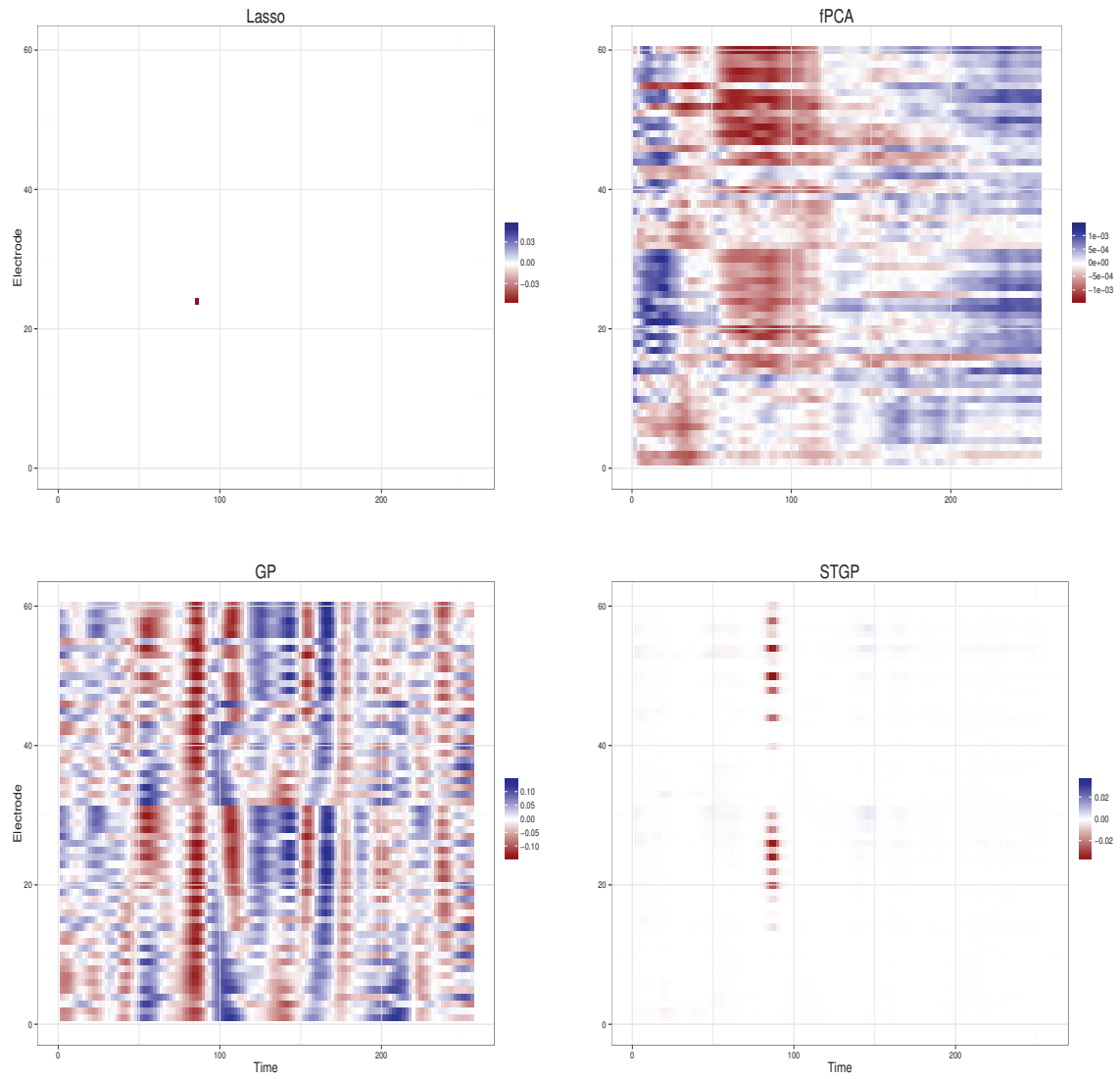
Figure 3: ROC curves for the five-fold cross validation of the EEG data. AUC refers to area under the curve



putation for these methods, we thin the time points by two, leaving 128 time points. While no model is uniformly superior, the area under the curve (AUC) corresponding to our approach is optimal among the alternatives we considered.

The differences between the models are further examined in the estimated β functions plotted in Fig. 4 (for now we ignore the spatial location of the electrodes and plot them using their ID number). The lasso solution is non-zero for a single spatiotemporal location, while the functional principal component analysis and Gaussian process methods lead to non-sparse and thus uninterpretable β estimates. In contrast, the soft-thresholded Gaussian process based estimate is near zero for the vast majority of locations, and isolates a subset of the electrodes near time point 86 as the most powerful predictors of alcoholism.

Figure 4: Estimated β for the EEG data. The GP and STGP estimates are posterior means.

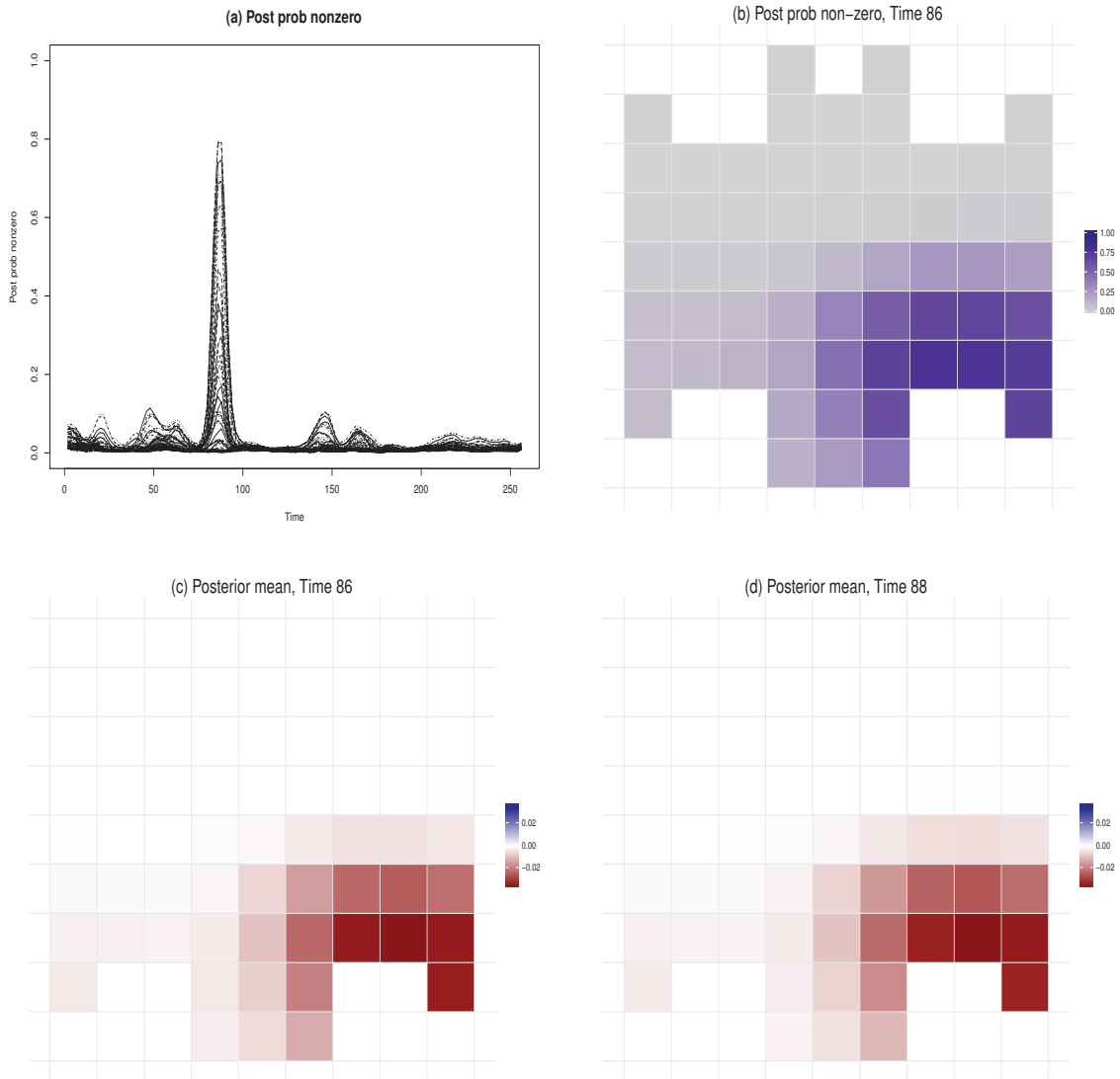


Our analysis indicates that EEG measurements at time $t = 86$, which roughly corresponds to 0.336 fraction of second, are predictive of the alcoholism status. This observation is further confirmed by the plot of the posterior probability of non-zero $\beta(s_j, t)$'s in Fig. 5a. This implies a delayed reaction to the stimulus; though such finding has to be confirmed with the investigators. To gain more insight into these findings, Fig. 5b-5d focus on a particular time and display the posterior mean and posterior probability of nonzero across the electrodes locations. They indicate that the right occipital/lateral part is the most predictive of the alcoholism status.

7 Discussions

In this work, we proposed a new class of Bayesian nonparametric prior model: the soft-thresholded Gaussian process, for variable selection in the scalar-on-image regression. It is completely different from the hard thresholded Gaussian process developed by Shi and Kang (2015) for the image-on-scalar regression. The soft-thresholded Gaussian process has two desired properties of Bayesian nonparametric models: 1) the prior support is large for a collection of piecewise smooth, sparse and continuous functions and 2) the posterior computation is feasible. We establish the posterior consistency for parameter estimation and variable selection for the normal response model. To the best of our knowledge, we are the first to obtain posterior consistency and the spatial variable selection consistency for scalar-on-image regression model. The regularity conditions for the theoretical development are not strong, the results hold even when the number of true predictors is greater than sample size. Also, we develop efficient posterior computation algorithms using the low rank approximation through the conditional autoregressive model. The posterior approximation computation algorithm is general and can be used for other models besides the normal response model. Our simulation studies and the analysis of EEG data both indicate

Figure 5: Summary of STGP analysis of the EEG data. Panel (a) plots the posterior probability of a nonzero $\beta(s, t)$; each electrode is a line plotted over time t . The remaining panels map either the posterior probability of a nonzero $\beta(s, t)$ or the posterior mean of $\beta(s, t)$ at individual time points.



that the proposed approach performs better than all existing methods in terms of model parameter estimations, predictions and scientific findings.

The proposed method generates a few feature directions that we consider to pursue. First, we plan to develop a more efficient posterior computation algorithm for analysis of voxel-level functional magnetic resonance imaging (fMRI) data, which typically contains 180,000 voxels for each subject. Any fast and scalable Gaussian processes approximation approach can be potentially applied to the soft-thresholded Gaussian process. For example, the recent ideas of nearest-neighbor Gaussian process approach by Datta et al. (2016) can be applied to our model. Also, it is of great interest to perform joint analysis of dataset involving multiple imaging modalities, such as fMRI, diffusion tensor imaging (DTI) and structural MRI. It is very challenging to model the dependence between the multiple imaging modality over space and to select the interactions between multiple modality imaging predictors in the scalar-on-image regression. The extension of the soft-thresholded Gaussian process can provide a potential solution to this problem. The basic idea is to introduce hierarchical latent Gaussian processes and different types of thresholding parameters for different modalities, leading to an hierarchical soft-thresholded Gaussian process as the prior model for the effects of interactions.

Acknowledgement

This research was supported partially by the National Institutes of Health grant R01 MH105561 (Kang), R01 NS085211 (Staicu) and R01 DE024984 (Reich), and the National Science Foundation grant DMS 0454942 (Staicu) and DMS 1513579 (Reich).

Supplementary material

Supplementary material contains the proofs of Lemmas 1, 3–5 and A1 – A6.

Appendix 1

Covering Number for Sieves

Lemma 6. *The ϵ -covering number $N(\epsilon, \Theta_n, \|\cdot\|_\infty)$ of Θ_n in the supremum norm satisfies*

$$\log N(\epsilon, \Theta_n, \|\cdot\|_\infty) \leq Cp_n^{1/(2\rho)} \epsilon^{-d/\rho}.$$

Test Constructions

Lemma 7. *Suppose Condition 3 holds for all s_j for $j = 1, \dots, p_n$ and K be the constant in Condition 3. Let $\nu > 0$ be a constant. For each integer n , let Λ_n be a collection of continuous functions, where each function $\gamma(s)$ is differentiable on a set \mathcal{D} that is dense in \mathcal{B} and $\sup_{s \in \mathcal{D}} |D\bar{\tau}\gamma| \leq p_n^{\|\bar{\tau}\|_1/2d} + \nu$, for $\|\bar{\tau}\|_1 \geq 0$. For each function $\gamma \in \Lambda_n$ and $\epsilon > 0$, define $\mathcal{V}_{\epsilon, \gamma} = \{s : |\gamma(s)| > \epsilon\}$. For all $n > N$ and $\gamma \in \Lambda_n$,*

$$\sum_{j=1}^{p_n} |\gamma(s_j)| \geq \frac{\lambda(\mathcal{V}_{\epsilon, \gamma})K\epsilon p_n}{2}.$$

Lemma 8. *Suppose Conditions 1 and 2 hold. For each $\epsilon > 0$, there exists an integer N and $r > 0$ such that, for all $n > N$ and for all $\beta \in \Theta_n$ such that $\|\beta - \beta_0\|_1 > \epsilon$, then*

$$\sum_{j=1}^{p_n} |\beta(s_j) - \beta_0(s_j)| > rp_n.$$

Lemma 9. *For any $0 < \epsilon < 1$ and $0 < r < \epsilon^2$, let*

$$A_n = \left\{ \sum_{i=1}^n p_n^{-1/2} \left| \sum_{j=1}^{p_n} X_{i,j} [\beta(s_j) - \beta_0(s_j)] \right| \geq nr \right\}.$$

There exists an integer N and constant $D > 0$ such that if for all $n > N$ and for all $\beta \in \Theta_n$,

$$\Pi \left[p_n^{-1/2} \left| \sum_{j=1}^{p_n} X(s_j) [\beta(s_j) - \beta_0(s_j)] \right| > \epsilon \right] > \epsilon,$$

then

$$\Pi [A_n^C] \leq \exp(-Dn) \quad \text{and} \quad \Pi \left[\bigcup_{m=1}^{\infty} \bigcap_{n=m}^{\infty} A_m \right] = 1.$$

Lemma 10. Suppose $\alpha_0^v = (\alpha_{0,1}, \dots, \alpha_{0,q})^T$ and σ_0^2 are known. The test statistic for the hypothesis testing problem

$$H_0 : \beta = \beta_0 \in \Theta, \quad \text{and} \quad H_1 : \beta = \beta_1 \in \Theta.$$

is give by

$$\Psi_n[\beta_0, \beta_1] = I \left[\sum_{i=1}^n \delta_i \left(\frac{Y_i - \eta_{i,0}}{\sigma_0} \right) > 2n^{v+1/2} \right],$$

where

$$\eta_{i,m} = \sum_{k=1}^q \alpha_{0,k} W_{i,k} + p_n^{-1/2} \sum_{j=1}^{p_n} \beta_m(s_j) X_{i,j},$$

for $m = 0, 1$, $\delta_i = 2I[\eta_{i,1} > \eta_{i,0}] - 1$ and $v_0/2 < v < 1/2$. Then for any $r > 0$, there exist constants C_0, C_1, N and $r_0 > 0$ such that for any β_0 and β_1 satisfy $\sum_{j=1}^{p_n} |\beta_1(s_j) - \beta_0(s_j)| > rp_n$, for any $n > N$, we have

$$E_{\beta_0}[\Psi_n(\beta_0, \beta_1)] \leq C_0 \exp(-2n^{2v}).$$

and for any β with $\|\beta - \beta_1\|_{\infty} < r_0/\{4c_{\max}^{1/2}\}$,

$$E_{\beta}[1 - \Psi_n(\beta_0, \beta_1)] \leq C_0 \exp(-C_1 n).$$

Appendix 2

Proofs of Lemma 2

Proof. For any $\lambda_0 > 0$, set $\alpha(s) = \beta_0(s) + \lambda_0$ for $s \in \bar{\mathcal{R}}_1$ and $\alpha(s) = \beta_0(s) - \lambda_0$ for $s \in \bar{\mathcal{R}}_{-1}$. Then by condition (C1), $\alpha(s)$ is smooth over $\bar{\mathcal{R}}_1 \cup \bar{\mathcal{R}}_{-1}$, i.e.

$$\alpha(s)I[s \in \bar{\mathcal{R}}_1 \cup \bar{\mathcal{R}}_{-1}] \in \mathcal{C}^{\rho}(\bar{\mathcal{R}}_1 \cup \bar{\mathcal{R}}_{-1}).$$

Next, we define $\alpha(s)$ on another closed subset of \mathcal{B} . Since \mathcal{B} is compact, $\partial\mathcal{R}_k$ for $k = -1, 1$ is also compact. For any $\epsilon > 0$ and each $t \in \mathcal{B}$, define an open ball $B(t, r) = \{s : \|t - s\|_2 < r\}$, where $\|\cdot\|_2$ is the Euclidean norm. For $k = -1, 1$, note that

$$\partial\mathcal{R}_k \subseteq \bigcup_{t \in \partial\mathcal{R}_k} B(t, r),$$

Since $\partial\mathcal{R}_1 \cup \partial\mathcal{R}_{-1}$ is compact, there exist $t_l \in \partial\mathcal{R}_1 \cup \partial\mathcal{R}_{-1}$, for $1 \leq l \leq L$, such that

$$\partial\mathcal{R}_{-1} \subseteq \bigcup_{l=1}^{L_0} B(t_l, r), \quad \partial\mathcal{R}_1 \subseteq \bigcup_{l=L_0+1}^L B(t_l, r)$$

Let $\mathcal{R}_0^*(r) = \mathcal{R}_0 - \bigcup_{l=1}^L B(t_l, r)$, then $\mathcal{R}_0^* \subseteq \mathcal{R}_0 - \partial\mathcal{R}_1 \cup \partial\mathcal{R}_{-1}$. Note that $\mathcal{R}_0 - \partial\mathcal{R}_1 \cup \partial\mathcal{R}_{-1}$ is a non-empty open set, $\mathcal{R}_0^*(r)$ is its closed subset and $\mathcal{R}_0^*(r)$ will increase as r decreases. There exists an r_0 , $0 < r_0 < 1$, such that $\mathcal{R}_0^*(r_0) \neq \emptyset$ and $\left(\bigcup_{l=1}^{L_0} B(t_l, r_0)\right) \cap \left(\bigcup_{l=L_0+1}^L B(t_l, r_0)\right) = \emptyset$. The latter fact is due to $\mathcal{R}_1 \cap \mathcal{R}_{-1} = \emptyset$. Since $\mathcal{R}_1 \cup \mathcal{R}_{-1}$ is bounded and $\alpha \in \mathcal{C}^\rho(\mathcal{R}_1 \cup \mathcal{R}_{-1})$, then $M = \max_{0 < \|\bar{\tau}\|_1 \leq \rho} \sup_{t \in \mathcal{R}_1 \cup \mathcal{R}_{-1}} |D^{\bar{\tau}}\alpha(t)| < \infty$. Take $r = \min\{\lambda_0 / \{2M(\rho + 1)^d + 1\}, r_0\}$. Define $\alpha(s) = 0$ if $s \in \mathcal{R}_0^*(r)$. Then $\alpha(s)$ is well defined on a closed set $\mathcal{R}^* = \mathcal{R}_0^* \cup \bar{\mathcal{R}}_1 \cup \bar{\mathcal{R}}_{-1}$, where $\mathcal{R}_0^* = \mathcal{R}_0^*(r)$.

Define a function

$$\phi(s, t) = \sum_{\|\bar{\tau}\|_1 \leq \rho} \frac{D^{\bar{\tau}}\alpha(t)}{\bar{\tau}!} (s - t)^{\bar{\tau}} \quad (7)$$

$$= \alpha(t) + \sum_{0 < \|\bar{\tau}\|_1 \leq \rho} \frac{D^{\bar{\tau}}\alpha(t)}{\bar{\tau}!} (s - t)^{\bar{\tau}} \quad (8)$$

when $t \in \partial\mathcal{R}_1 \cup \partial\mathcal{R}_{-1}$ and $s \in B(t, r_0)$,

$$|\phi(s, t)| \leq |\lambda_0| + \left| \sum_{0 < \|\bar{\tau}\|_1 \leq \rho} \frac{D^{\bar{\tau}}\alpha(t)}{\bar{\tau}!} (s - t)^{\bar{\tau}} \right| \leq \lambda_0 + 2M(\rho + 1)^d r_0$$

when $t \in \partial\mathcal{R}_0^*(r_0)$ and $\|s - t\| < r_0$,

$$|\phi(s, t)| \leq 2M(\rho + 1)^d r_0.$$

Define

$$\psi(t) = \sum_{l=1}^L \psi(t, t_l).$$

where

$$\psi(t, t_l) = C_l \exp \left\{ -\frac{1}{1 - \|t - t_l\|_2/r} \right\} I[\|t - t_l\|_2 < r].$$

We choose C_l for $l = 1, \dots, L$ such that

$$\sum_{l=1}^L \int_{B(t_l, r)} \psi(t, t_l) dt = 1, \quad \text{and} \quad \sum_{l=L_0+1}^L \int_{B(t_l, r)} \psi(t, t_l) dt < 1 - \frac{2M(\rho+1)^d r}{\lambda_0}.$$

We construct $\tilde{\beta}_0(s)$ by extending $\alpha(s)$ from \mathcal{R}^* to the whole domain \mathcal{B} . Let

$$\tilde{\beta}_0(s) = \begin{cases} \int_{\partial \mathcal{R}^*} \phi(s, t) \psi(t) dt, & s \in \mathcal{B} - \mathcal{R}^* \\ \alpha(s), & s \in \mathcal{R}^* \end{cases} \quad (9)$$

Note that

$$\begin{aligned} & \left| \int_{\partial \mathcal{R}^*} \phi(s, t) \psi(t) dt \right| \\ & \leq \sum_{l=1}^L \int_{\partial \mathcal{R}^* \cap B(t_l, r)} |\phi(s, t)| \psi(s, t) dt \\ & \leq \sum_{l=1}^L \left(\int_{\partial \mathcal{R}_0^* \cap B(t_l, r)} |\phi(s, t)| \psi(s, t) dt + \int_{\partial(\mathcal{R}_1 \cup \mathcal{R}_{-1}) \cap B(t_l, r)} |\phi(s, t)| \psi(s, t) dt \right) \\ & < 2M(\rho+1)^d r (1 - w_1) + (\lambda_0 + 2M(\rho+1)^d r) w_1 < \lambda_0 \end{aligned}$$

where

$$w_1 = \sum_{l=L_0+1}^L \int_{B(t_l, r)} \psi(t, t_l) dt < 1 - \frac{2M(\rho+1)^d r}{\lambda_0}.$$

Next, we show that

$$\lim_{s \rightarrow s_0} D^{\bar{\tau}} \tilde{\beta}_0(s) = D^{\bar{\tau}} \alpha(s_0), \quad \text{for any } s_0 \in \partial \mathcal{R}^* \text{ and } \bar{\tau} \text{ with } \|\bar{\tau}\|_1 \leq \rho.$$

For any ϵ , $0 < \epsilon < 1$, since $D^{\bar{\tau}} \alpha$ is continuous over \mathcal{R}^* , there exists some $\delta_1 > 0$, for all t such that $\|t - s_0\| < \delta_1$, we have $|D^{\bar{\tau}} \alpha(t) - D^{\bar{\tau}} \alpha(s_0)| < \epsilon/2$. Take $\delta <$

$\min\{\epsilon/\{2(\rho+1)^d M\}, r, \delta_1\}$, as long as $\|s_0 - s\| < \delta$, we have

$$\begin{aligned} |D^{\bar{\tau}}\tilde{\beta}_0(s) - D^{\bar{\tau}}\tilde{\alpha}(s_0)| &\leq \int_{\partial\mathcal{R}^*} |D^{\bar{\tau}}\alpha(t) - D^{\bar{\tau}}\alpha(s_0)|\psi(t)dt \\ &\quad + \sum_{\|\bar{\tau}'\|_1 \geq \|\bar{\tau}\|_1, \bar{\tau}' \neq \bar{\tau}} \int_{\partial\mathcal{R}^*} \frac{|D^{\bar{\tau}'}\alpha(t)|}{\bar{\tau}'!} |(s-t)^{\bar{\tau}'}|\psi(t)dt \\ &< \frac{\epsilon}{2} + (\rho+1)^d M\delta < \epsilon. \end{aligned}$$

By condition 2 and the definition of $\alpha(s)$, we have

$$\alpha(s) = \lambda_0, \text{ for } s \in \partial\mathcal{R}_1, \quad \text{and} \quad \alpha(s) = -\lambda_0, \text{ for } s \in \partial\mathcal{R}_{-1} \quad (10)$$

□

Proof of Theorem 2

Proof. The proof can be done by verifying the conditions in Theorem A.1 of Choudhuri et al. (2004). Specifically, we have the condition on prior positivity of neighborhoods by Lemma 3. By Lemma A4, Lemma 5 and Condition 1, as $n \rightarrow \infty$,

$$\begin{aligned} E_{\beta_0}\Psi_n &\rightarrow 0, \\ \sup_{\beta \in \mathcal{U}_\epsilon^C \cap \Theta_n} E_\beta[1 - \Psi_n] &\leq C_0 \exp(-C_1 n), \\ \Pi(\Theta_n^C) &\leq K \exp(-bp_n^{1/d}) \leq K \exp(-C_3 n). \end{aligned}$$

This establishes the condition on the existence of tests. □

Proof of Theorem 3

Proof. Define $\mathcal{U}_\epsilon = \{\beta \in \Theta : \|\beta - \beta_0\|_1 < \epsilon\}$. Let $\mathcal{R}_0 = \{s : \beta_0(s) = 0\}$, $\mathcal{R}_1 = \{s : \beta_0(s) > 0\}$ and $\mathcal{R}_{-1} = \{s : \beta_0(s) < 0\}$.

For any $\mathcal{A} \subseteq \mathcal{B}$ and any integer $m \geq 1$, define

$$\mathcal{F}_m(\mathcal{A}) = \left\{ \beta \in \Theta : \int_{\mathcal{A}} |\beta(s) - \beta_0(s)| ds < \frac{1}{m} \right\}.$$

Then $\mathcal{F}_{m+1}(\mathcal{A}) \subseteq \mathcal{F}_m(\mathcal{A})$ for all m and $\mathcal{F}_m(\mathcal{B}) \subseteq \mathcal{F}_m(\mathcal{A})$.

Consider

$$\mathcal{F}_m(\mathcal{R}_0) = \left\{ \beta \in \Theta : \int_{\mathcal{R}_0} |\beta(s)| ds < \frac{1}{m} \right\}.$$

By Theorem 2, note that $\mathcal{U}_{1/m} = \mathcal{F}_m(\mathcal{B})$, thus,

$$\Pi(\mathcal{F}_m(\mathcal{R}_0) \mid D_n) \geq \Pi(\mathcal{U}_{1/m} \mid D_n) \rightarrow 1,$$

as $n \rightarrow \infty$ in $P_{\beta_0}^n$ probability. Also,

$$\{\beta(s) = 0, \text{ for all } s \in \mathcal{R}_0\} = \left\{ \int_{\mathcal{R}_0} |\beta(s)| ds = 0 \right\} = \bigcap_{m=1}^{\infty} \mathcal{F}_m(\mathcal{R}_0).$$

By the monotone continuity of probability measure, we have

$$\Pi\{\beta(s) = 0, \text{ for all } s \in \mathcal{R}_0 \mid D_n\} = \lim_{m \rightarrow \infty} \Pi(\mathcal{F}_m(\mathcal{R}_0) \mid D_n) = 1. \quad (11)$$

as $n \rightarrow \infty$ in $P_{\beta_0}^n$ probability.

For any $s_0 \in \mathcal{R}_1$ and any integer $m \geq 1$, by Condition 2.3, there exists $\delta_0 > 0$, such that for any $s_1 \in B(s_0, \delta_0) = \{s : \|s_1 - s_0\|_1 < \delta_0\}$, such that

$$|\beta(s_1) - \beta(s_0)| < \frac{1}{2m}.$$

By Definition 2, \mathcal{R}_1 is an open set, then there exists $\delta_1 > 0$, such that $B(s_0, \delta_1) \subseteq \mathcal{R}_1$.

Taking $\delta = \min\{\delta_1, \delta_0\} > 0$, we have that

$$\begin{aligned} & \left\{ \beta(s_0) > -\frac{1}{m}, \text{ for all } s_0 \in \mathcal{R}_1 \right\} \\ & \supseteq \left\{ \beta(s_0) > \beta(s_1) - \frac{1}{2m} \text{ and } \beta(s_1) > -\frac{1}{2m}, \text{ for some } s_1 \in B(s_0, \delta), \text{ for all } s_0 \in \mathcal{R}_1 \right\} \\ & \supseteq \left\{ \int_{B(s_0, \delta)} \beta(s) ds > -\frac{1}{2m}, \text{ for all } s_0 \in \mathcal{R}_1 \right\} \\ & \supseteq \left\{ \int_{B(s_0, \delta)} \beta(s) ds > \int_{B(s_0, \delta)} \beta_0(s) ds - \frac{1}{2m}, \text{ for all } s_0 \in \mathcal{R}_1 \right\} \\ & \supseteq \mathcal{F}_{2m}[B(s_0, \delta)] \supseteq \mathcal{U}_{1/2m} \end{aligned}$$

thus,

$$\Pi \left(\beta(s_0) > -\frac{1}{m}, \text{ for all } s_0 \in \mathcal{R}_1 \mid D_n \right) \geq \Pi(\mathcal{U}_{1/2m} \mid D_n) \rightarrow 1,$$

as $n \rightarrow \infty$ in $P_{\beta_0}^n$ probability. By the monotone continuity of probability measure, we have

$$\Pi \{ \beta(s) > 0, \text{ for all } s \in \mathcal{R}_1 \mid D_n \} = \lim_{m \rightarrow \infty} \Pi \left(\beta(s_0) > -\frac{1}{m}, \text{ for all } s_0 \in \mathcal{R}_1 \mid D_n \right) \rightarrow 1. \quad (12)$$

as $n \rightarrow \infty$ in $P_{\beta_0}^n$ probability. Similar arguments can be made to show

$$\Pi \{ \beta(s) < 0, \text{ for all } s \in \mathcal{R}_{-1} \mid D_n \} \rightarrow 1. \quad (13)$$

as $n \rightarrow \infty$ in $P_{\beta_0}^n$ probability. Combing (11) – (13) completes the proof. \square

References

- Arnold, T. B. and Tibshirani, R. J. (2014), *genlasso: Path algorithm for generalized lasso problems*, r package version 3.0.2.
- Banerjee, S., Carlin, B. P., and Gelfand, A. E. (2004), *Hierarchical modeling and analysis for spatial data*, Boca Rotan, FL: Chapman & Hall/CRC.
- Boehm Vock, L. F., Reich, B. J., Fuentes, M., and Dominici, F. (2014), “Spatial variable selection methods for investigating acute health effects of fine particulate matter components,” *Biometrics*, 71, 167–177.
- Choudhuri, N., Ghosal, S., and Roy, A. (2004), “Bayesian estimation of the spectral density of a time series,” *Journal of the American Statistical Association*, 99, 1050–1059.
- Crainiceanu, C., Reiss, P., Goldsmith, J., Huang, L. and Huo, L., and Scheipl, F. (2014), *refund: Regression with functional data*, r package version 3.0.2.
- Cressie, N. (1993), *Statistics for Spatial Data*, New York: Wiley-Interscience.

- Datta, A., Banerjee, S., Finley, A. O., and Gelfand, A. E. (2016), “Hierarchical nearest-neighbor Gaussian process models for large geostatistical datasets,” *Journal of the American Statistical Association*.
- Gelfand, A. E., Diggle, P. J., Fuentes, M., and Guttorp, P. (2010), *Handbook of Spatial Statistics*, New York: Chapman & Hall/CRC.
- Ghosal, S. and Roy, A. (2006), “Posterior consistency of Gaussian process prior for nonparametric binary regression,” *The Annals of Statistics*, 2413–2429.
- Goldsmith, J., Huang, L., and Crainiceanu, C. M. (2014), “Smooth scalar-on-image regression via spatial Bayesian variable selection,” *Journal of Computational and Graphical Statistics*, 23, 46–64.
- Hastie, T. and Efron, B. (2013), *lars: Least angle regression, lasso and forward stage-wise*, r package version 3.0.2.
- Higdon, D., Swall, J., and Kern, J. (1999), “Non-Stationary Spatial Modeling,” in *Bayesian Statistics 6 - Proceedings of the Sixth Valencia Meeting*, J.M. Bernardo, J.O. Berger, A.P. Dawid, and A.F.M. Smith, (editors). Clarendon Press - Oxford, pp. 761–768.
- Hung, H. and Wang, C.-C. (2013), “Matrix variate logistic regression model with application to EEG data,” *Biostatistics*, 14, 189–202.
- Li, B., Kim, M. K., and Altman, N. (2010), “On dimension folding of matrix-or array-valued statistical objects,” *The Annals of Statistics*, 1094–1121.
- Li, F., Zhang, T., Wang, Q., Gonzalez, M., Maresh, E., and Coan, J. (2015), “Spatial Bayesian variable selection and grouping in high-dimensional scalar-on-image regressions,” *Annals of Applied Statistics*, 9, 687–713.

- Møller, J., Pettitt, A., Berthelsen, K., and Reeves, R. (2006), “An efficient Markov chain Monte Carlo method for distributions with intractable normalising constants,” *Biometrika*, 93, 451–458.
- Nelsen, R. B. (1999), *An introduction to copulas*, New York: Springer-Verlag.
- Nychka, D., Bandyopadhyay, S., Hammerling, D. M., Lindgren, F., and Sain, S. (2015), “A multi-resolution Gaussian process model for the analysis of large spatial data sets,” *Journal of Computational and Graphical Statistics*, 24, 579–599.
- R Core Team (2013), *R: A Language and Environment for Statistical Computing*, R Foundation for Statistical Computing, Vienna, Austria.
- Reich, B. J., Hodges, J. S., and Carlin, B. P. (2007), “Spatial analysis of periodontal data using conditionally autoregressive priors having two types of neighbor relations,” *Journal of the American Statistical Association*, 102, 44–55.
- Reiss, P. T. and Ogden, R. T. (2010), “Functional generalized linear models with images as predictors,” *Biometrics*, 66, 61–69.
- Shi, R. and Kang, J. (2015), “Thresholded Multiscale Gaussian Processes with Application to Bayesian Feature Selection for Massive Neuroimaging Data,” *arXiv preprint arXiv:1504.06074*.
- Smith, M. and Fahrmeir, L. (2007), “Spatial Bayesian variable selection with application to functional magnetic resonance imaging,” *Journal of the American Statistical Association*, 102, 417–431.
- Tibshirani, R. (1996), “Regression shrinkage and selection via the lasso,” *Journal of the Royal Statistical Society. Series B (Methodological)*, 267–288.

- Tibshirani, R., Saunders, M., Rosset, S., Zhu, J., and Knight, K. (2005), “Sparsity and smoothness via the fused lasso,” *Journal of the Royal Statistical Society: Series B*, 67, 91–108.
- Tibshirani, R. J. and Taylor, J. (2011), “The solution path of the generalized lasso,” *Annals of Statistics*, 39, 1335–1371.
- Wang, X. and Zhu, H. (2015), “Generalized scalar-to-image regression models via total variation,” *Submitted*.
- Xiao, L., Li, Y., and Ruppert, D. (2013), “Fast bivariate P-splines: The sandwich smoother,” *Journal of the Royal Statistical Society: Series B*, 75, 577–599.
- Zhou, H. and Li, L. (2014), “Regularized matrix regression,” *Journal of the Royal Statistical Society: Series B (Statistical Methodology)*, 76, 463–483.